Cold Nuclear Matter J/ψ Production with SeaQuest

R. Vogt

Lawrence Livermore National Laboratory, Livermore, CA 94551, USA
Physics and Astronomy Department, UC Davis, Davis, CA 95616, USA

based on:
RV, arXiv:2101.02858, Phys. Rev. C in press

Figure 1: This work was performed under the auspices of the U.S. Department of Energy by Lawrence Livermore National Laboratory under Contract DE-AC52-07NA27344 and the LLNL-LDRD Program under Project No. 21-LW-034.

Intrinsic Charm is Long-standing Puzzle in QCD

An intrinsic charm component of the hadron wavefunction, $|uudc\bar{c}\rangle$, was first proposed by Brodsky, Hoyer, Peterson and Sakai in the 1980's

If this state is the dominant Fock component, its invariant mass is minimized, giving the charm quarks a larger fraction of the hadron momentum and leading to enhanced charm production in the forward region

A number of experimental hints have been seen, no conclusive results

- **EMC charm structure function, F_2^c, large at largest x and highest Q^2 measured in experiment**
- **Leading charm asymmetries (D^- over D^+ in $\pi^- p$ interactions) consistent with intrinsic charm predictions**
- **Double J/ψ production observed at high pair x_F by NA3**
- **Forward charm production observed in many fixed-target experiments**
- **Proposed explanation of high energy astrophysical neutrino rate at Ice Cube (Brodsky and Laha)**

At colliders, forward x_F pushed to very high rapidity and detection is less likely, lower energy, fixed-target configurations better for discovery measurement

SeaQuest is Ideal for Intrinsic Charm Searches

SeaQuest experimantl setup directs a 120 GeV proton beam on proton and nuclear targets: $p+p$**,** $p+\mathrm{d}$**,** $p+\mathrm{C}$**,** $p+\mathrm{Fe}$ **and** $p+\mathrm{W}$

Detector coverage for J/ψ **is in sweet spot for intrinsic charm:** $0.4 < x_F < 0.95$ **and** $p_T < 2.3$ **GeV**

SeaQuest will report nuclear suppression factor: $pA/p\mathrm{d}$ **ratio**

Results can be tested against calculations for the E866/NuSea experiment also at FNAL but at higher energy: they used an 800 GeV proton beam on proton, Be, Fe and W targets

E866 covered full forward x_F **range:** $-0.1 < x_F < 0.95$ **and also looked at the** p_T **dependence in 3 different** x_F **bins: low** x_F $(-0.1 \leq x_F \leq 0.3)$**; intermediate** x_F $(0.2 \leq x_F \leq 0.6)$**; high** x_F $(0.3 \leq x_F \leq 0.95)$

E866 results reported as α **in** $\sigma_{pA} = A^{\alpha}\sigma_{ppp}$ **– provides less information because** α **is averaged over all targets; nuclear suppression factor is more direct**

Components of Model Calculation

Nuclear suppression factor includes both perturbative cross section and production by intrinsic charm:

$$\begin{aligned} \sigma_{pA} &= \sigma_{\rm CEM}(pA) + \sigma_{\rm ic}^{J/\psi}(pA) \\ \sigma_{p{\rm d}} &= 2\sigma_{\rm CEM}(pp) + \sigma_{\rm ic}^{J/\psi}(pA) \end{aligned}$$

$\sigma_{\rm CEM}$ is the production cross section computed at NLO in the color evaporation model for $p+p$ and $p+A$ interactions

$\sigma_{\rm ic}^{J/\psi}$ is intrinsic charm production cross section including the probability for an intrinsic charm contribution to the proton wavefunction

Components of all terms are discussed in detail in the following slides

Charmonium Production in Color Evaporation Model

The CEM at NLO is employed for the perturbative production cross section:

$$\sigma_{\rm CEM}(pp) = F_C \sum_{i,j} \int_{4m^2}^{4m_H^2} ds \int dx_1\, dx_2\ F_i^p(x_1, \mu_F^2, k_{T_1})\ F_j^p(x_2, \mu_F^2, k_{T_2})\ \hat{\sigma}_{ij}(\hat{s}, \mu_F^2, \mu_R^2)$$

Parton densities factorized into longitudinal (CT10) and a k_T-dependent component to implement k_T broadening a la low p_T resummation

$$F^p(x, \mu_F^2, k_T) = f^p(x, \mu_F^2) G_p(k_T)$$

$$\begin{aligned} g_p(k_T) &= G_p(k_{T_1}) G_p(k_{T_2}) \\ g_p(k_T) &= \frac{1}{\pi \langle k_T^2 \rangle_p} \exp(-k_T^2/\langle k_T^2 \rangle_p) \end{aligned}$$

Broadening with proton beam assumed energy dependent, $n = 12$ from J/ψ data; at $\sqrt{s_{NN}} = 15.4$ GeV, $\langle k_T^2 \rangle_p = 0.97$ GeV^2

$$\langle k_T^2 \rangle_p = \left[1 + \frac{1}{n} \ln \left(\frac{\sqrt{s_{NN}}(\text{GeV})}{20\,\text{GeV}} \right) \right]\ \text{GeV}^2$$

Uncertainty band on cross section set by:

$$\begin{aligned} \frac{d\sigma_{\rm max}}{dX} &= \frac{d\sigma_{\rm cent}}{dX} + \sqrt{\left(\frac{d\sigma_{\mu,\rm max}}{dX} - \frac{d\sigma_{\rm cent}}{dX} \right)^2 + \left(\frac{d\sigma_{m,\rm max}}{dX} - \frac{d\sigma_{\rm cent}}{dX} \right)^2} \\ \frac{d\sigma_{\rm min}}{dX} &= \frac{d\sigma_{\rm cent}}{dX} - \sqrt{\left(\frac{d\sigma_{\mu,\rm min}}{dX} - \frac{d\sigma_{\rm cent}}{dX} \right)^2 + \left(\frac{d\sigma_{m,\rm min}}{dX} - \frac{d\sigma_{\rm cent}}{dX} \right)^2} \end{aligned}$$

J/ψ Distributions in CEM at $\sqrt{s_{NN}} = 15.4$ GeV

Uncertainty bands defined by $(m, \mu_F/m_T, \mu_R/m_T) = (1.27 \pm 0.09\,\mathrm{GeV}, 2.1^{+2.55}_{-0.85}, 1.6^{+0.11}_{-0.12})$**;** μ_F**, factorization scale, and** μ_R**, renormalization scale, defined relative to pair transverse mass:** $\mu_{F,R} \propto m_T = \sqrt{m^2 + p_T^2}$ **where** $p_T^2 = 0.5(p_{T_Q}^2 + p_{T_{\overline{Q}}}^2)$

Scale uncertainties set by $\{(\mu_F/m_T, \mu_F/m_T)\} = \{(C,C),\ (H,H),\ (L,L),\ (C,L),\ (L,C),\ (C,H),\ (H,C)\}$

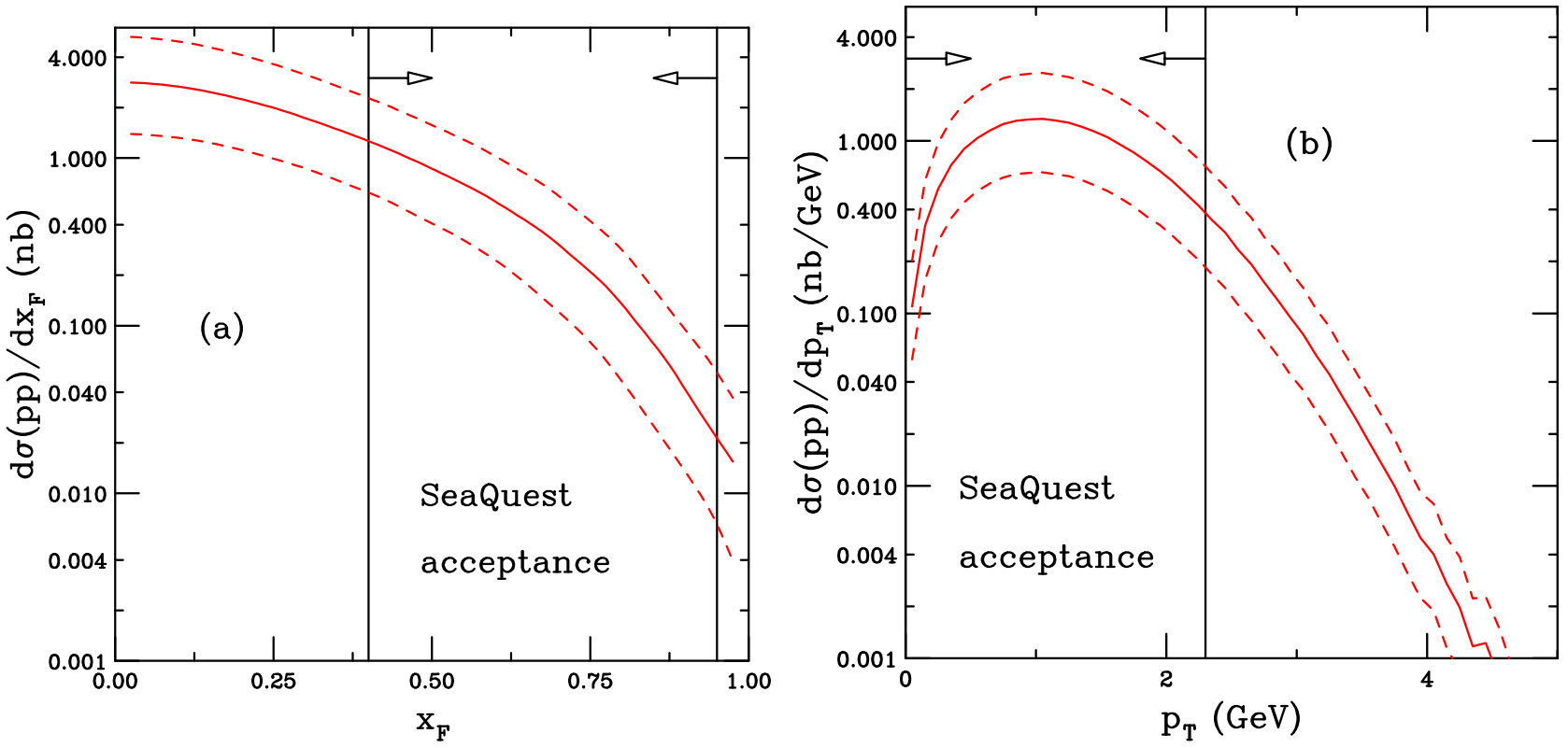

Figure 2: The J/ψ production cross sections in the CEM in $p+p$ collisions at $\sqrt{s} = 15.4$ GeV as a function of x_F (a) and p_T (b), integrated over all phase space, are shown. The solid curves show the central values while the dashed curves outline the upper and lower limits of the uncertainty band.

Cold Matter Effects on Perturbative Cross Section

Production cross section in a pA collision becomes

$$\sigma_{pA} = \sigma_{\rm CEM}(pA) = S_A^{\rm abs} F_C \sum_{i,j} \int_{4m^2}^{4m_H^2} ds \int dx_1\, dx_2\ F_i^p(x_1, \mu_F^2, k_T)\ F_j^A(x_2, \mu_F^2, k_T)\ \hat{\sigma}_{ij}(\hat{s}, \mu_F^2, \mu_R^2)$$

Survival probability for absorption of a (proto)charmonium state in nuclear matter

$$\begin{aligned}
\sigma_{pA} = \sigma_{pN} S_A^{\rm abs} &= \sigma_{pN} \int d^2b \int_{-\infty}^{\infty} dz\, \rho_A(b,z) S^{\rm abs}(b) \\
&= \sigma_{pN} \int d^2b \int_{-\infty}^{\infty} dz\, \rho_A(b,z) \exp\left\{ - \int_z^{\infty} dz' \rho_A(b,z') \sigma_{\rm abs}(z'-z) \right\}
\end{aligned}$$

Here the absorption cross section is assumed constant but note that prior experiments extracted an effective absorption cross section from A^α analysis with $\alpha = 1 - 9\sigma_{\rm abs}/(16\pi r_0^2)$ assuming no other nuclear effects

Nuclear parton densities

$$F_j^A(x_2, \mu_F^2, k_T) = R_j(x_2, \mu_F^2, A) f_j(x_2, \mu_F^2) G_A(k_T) \quad (1)$$

$$F_i^p(x_1, \mu_F^2, k_T) = f_i(x_1, \mu_F^2) G_p(k_T)\ . \quad (2)$$

For a deuteron target, $R_j \equiv 1$

$$g_A(k_T) = G_p(k_{T_1}) G_A(k_{T_2})\ , \quad (3)$$

$G_A(k_T)$ includes increased broadening in the nuclear target ($A > 2$)

k_T Broadening in Nuclei

k_T broadening in nuclei may arise from multiple scattering in the target, to implement broadening, a larger value of $\langle k_T^2 \rangle$ is used for nuclear targets

$$\langle k_T^2 \rangle_A = \langle k_T^2 \rangle_p + \delta k_T^2$$

δk_T^2 gives strength of broadening

$$\delta k_T^2 = (\langle \nu \rangle - 1)\Delta^2(\mu)$$

The broadening strength depends on the interaction scale:

$$\Delta^2(\mu) = 0.225 \frac{\ln^2(\mu/\mathrm{GeV})}{1 + \ln(\mu/\mathrm{GeV})} \mathrm{GeV}^2 \qquad \mu = 2m_c$$

Strength also depends on number of scatterings proton undergoes passing through nuclear target, $\langle \nu \rangle - 1$

$$\langle \nu \rangle = \sigma_{pp}^{\mathrm{in}} \frac{\int d^2b T_A^2(b)}{\int d^2b T_A(b)} = \frac{3}{2} \rho_0 R_A \sigma_{pp}^{\mathrm{in}}$$

T_A is the nuclear profile function, here $\rho_0 = 0.16/\mathrm{fm}^3$, $R_A = 1.2A^{1/3}$, and the inelastic $p + p$ cross section is $\sigma_{pp}^{\mathrm{in}} \sim 32$ mb

At the SeaQuest energy $\delta k_T^2 = 0.1$ (carbon), 0.25 (iron), and 0.39 GeV^2 (tungsten), giving $\langle k_T^2 \rangle_A = 1.07$, 1.22, and 1.36 GeV^2 respectively

Broadening increases at higher energies: $\langle k_T^2 \rangle_p$ is larger and the inelastic cross section, $\sigma_{pp}^{\mathrm{in}}$, also increases

Nuclear Modification of the Parton Densities

EPPS16 nuclear parton density modifications differentiate between u and d valence quarks and all sea quarks; 20 parameters give 40 error sets + 1 central set

Uncertainties are determined by calculating cross section for each A with all error sets, adding differences around central set for each parameter in quadrature

$$f_j^A(x_2, \mu_F^2) = R_j(x_2, \mu_F^2, A) f_j^p(x_2, \mu_F^2)$$

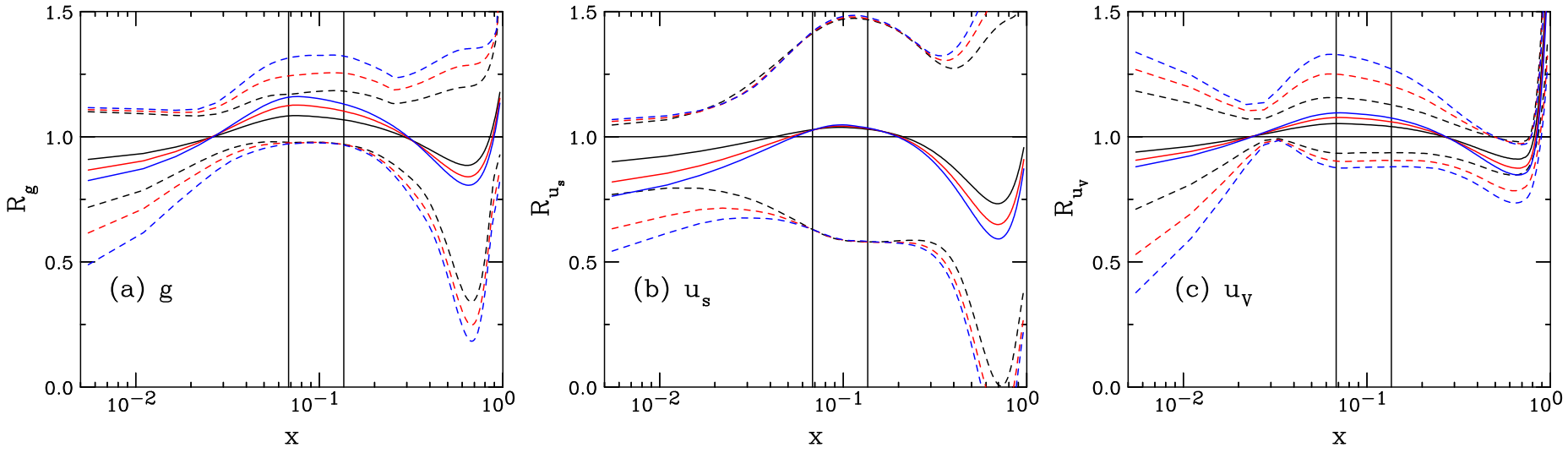

Figure 3: The EPPS16 ratios, with uncertainties, are shown at the scale of the J/ψ mass for gluons (a), the up sea quark distribution (b) and the valence up quark distribution (c) as a function of momentum fraction x. The central set is denoted by the solid curves while the dashed curves give the upper and lower limits of the uncertainty bands. The results are given for $A = 12$ (black), 56 (red) and 184 (blue). The vertical lines indicate the x range of the SeaQuest measurement, $0.068 < x < 0.136$.

Interplay of Shadowing and Absorption

Depending on x values probed, shadowing can enhance or reduce absorption cross section needed to describe data

Absorption alone always gives less than linear A dependence ($\alpha < 1$)

For SPS energies, $17.3 \leq \sqrt{s_{NN}} \leq 29$ GeV, rapidity range covered is in EMC and antishadowing region, $\alpha > 1$ with no absorption

Adding shadowing to absorption in the SPS energy region requires a larger absorption cross section is needed to maintain agreement with data

For $\sqrt{s_{NN}} \geq 38$ GeV, x in shadowing regime, thus $\alpha < 1$ with shadowing alone in forward region, reducing needed absorption cross section to $\sigma_{\rm abs} \sim 0$ at the LHC

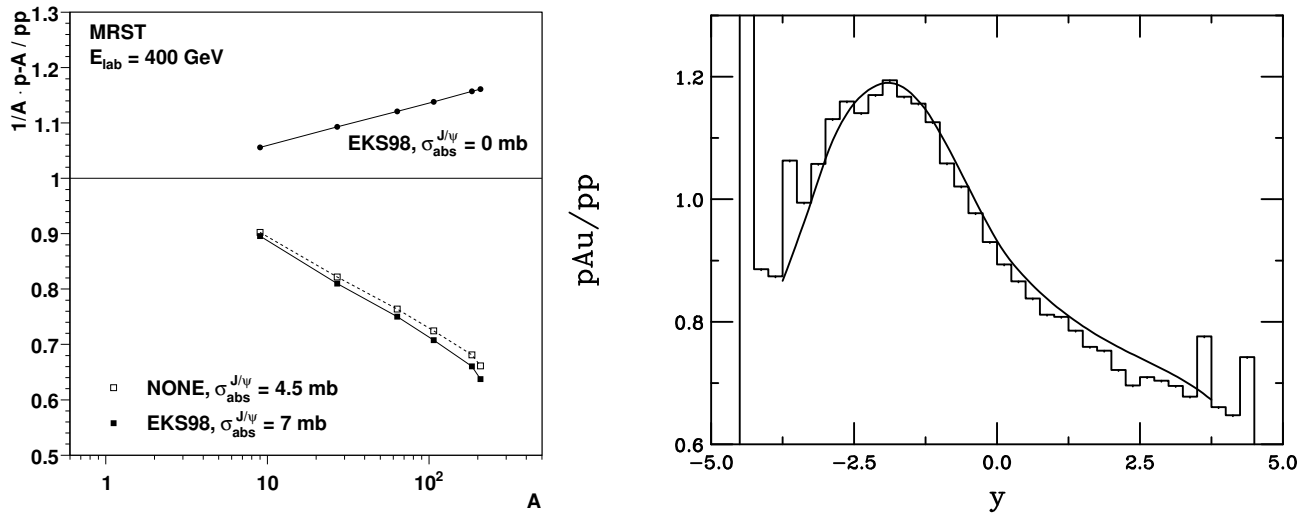

Figure 4: **(Left) Illustration of the interplay between shadowing and absorption. [C. Lourenco, H. K. Woehri and RV, JHEP 0902 (2009) 014.] (Right) Comparison of LO and NLO shadowing ratios.**

Energy Dependence of $\sigma_{\rm abs}^{J/\psi}$

At midrapidity, systematic decrease of absorption cross section with center of mass energy, independent of shadowing, trend continues at RHIC and above

$\sigma_{\rm abs}^{J/\psi}(y_{\rm cms}=0)$ extrapolated to 158 GeV is significantly larger than measured at 450 GeV, underestimating "normal nuclear absorption" in SPS heavy-ion data

Calculations confirmed by NA60 pA measurements at 158 GeV showing stronger absorption with L, from these results, $\sigma_{\rm abs} = 9$ mb is used for SeaQuest calculations

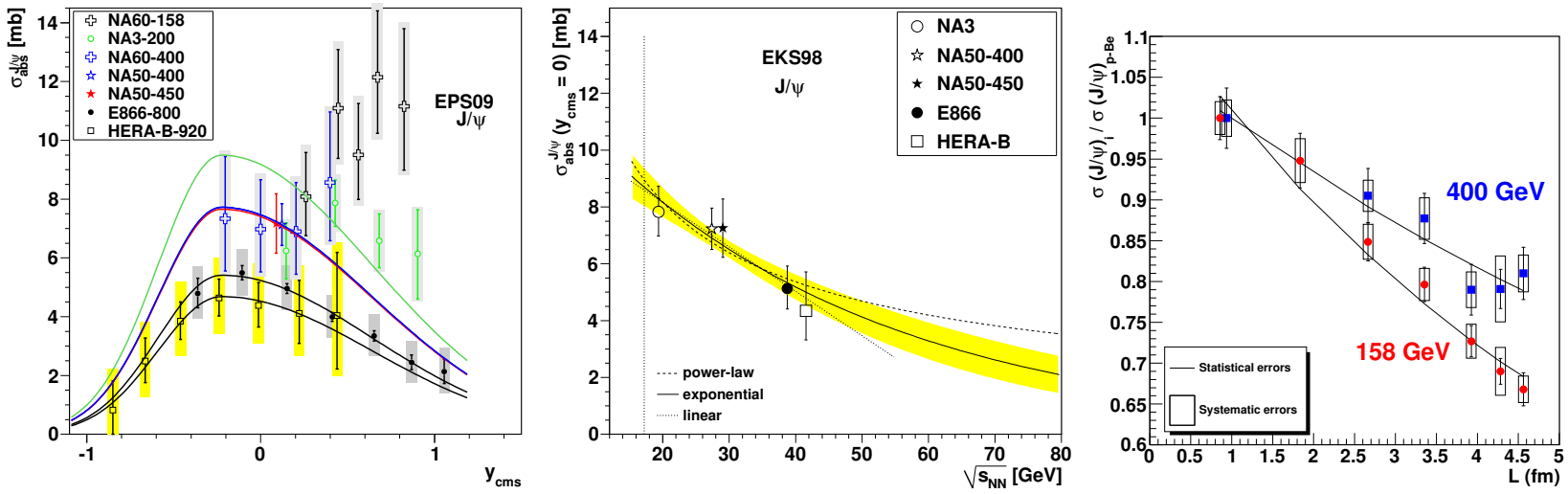

Figure 5: Left: Dependence of $\sigma_{\rm abs}^{J/\psi}$ on $y_{\rm cms}$ for all available data sets including EPS09 shadowing. The shape of the curves is fixed by the E866 and HERA-B data. [Lourenço, RV, Wöhri] Middle: The extracted energy dependence of $\sigma_{\rm abs}^{J/\psi}$ at midrapidity for power law (dashed), exponential (solid) and linear (dotted) approximations to $\sigma_{\rm abs}^{J/\psi}(y=0,\sqrt{s_{NN}})$ using the EKS98 shadowing parameterization with the CTEQ61L parton densities. The band around the exponential curve indicates the uncertainty in the extracted cross sections at $x_F \sim 0$ from NA3, NA50 at 400 and 450 GeV, E866 and HERA-B. The vertical dotted line indicates the energy of the Pb+Pb and In+In collisions at the CERN SPS. [Lourenço, RV, Wöhri] Right: The J/ψ cross section ratios for pA collisions at 158 GeV (circles) and 400 GeV (squares), as a function of L, the mean thickness of nuclear matter traversed by the J/ψ.

Intrinsic Charm

Probability distribution of five-particle Fock state of the proton:

$$dP_{\mathrm{ic}\,5} = P^0_{\mathrm{ic}\,5} N_5 \int dx_1 \cdots dx_5 \int dk_{x\,1} \cdots dk_{x\,5} \int dk_{y\,1} \cdots dk_{y\,5} \frac{\delta(1 - \sum_{i=1}^5 x_i)\delta(\sum_{i=1}^5 k_{x\,i})\delta(\sum_{i=1}^5 k_{y\,i})}{(m_p^2 - \sum_{i=1}^5 (\widehat{m}_i^2/x_i))^2}$$

$i = 1, 2, 3$ are u, u, d light quarks, 4 and 5 are c and $\overline{c}$, N_t normalizes the probability to unity and P^0_{ic} scales the normalized probability to the assumed intrinsic charm content: 0.1%, 0.31% and 1% are used to represent the range of probabilities assumed previously

The IC cross section is determined from soft interaction scale breaking coherence of the Fock state, $\mu^2 = 0.1$ GeV^2

$$\sigma_{\mathrm{ic}}(pp) = P_{\mathrm{ic}\,5} \sigma^{\mathrm{in}}_{pN} \frac{\mu^2}{4\widehat{m}_c^2}$$

The J/ψ cross section from intrinsic charm is then obtained by multiplying by the normalization factor for the CEM to the J/ψ

$$\sigma^{J/\psi}_{\mathrm{ic}}(pp) = F_C \sigma_{\mathrm{ic}}(pp)$$

The A depedence is

$$\sigma^{J/\psi}_{\mathrm{ic}}(pA) = \sigma^{J/\psi}_{\mathrm{ic}}(pp)\, A^{\beta}$$

where $\beta = 0.71$ for a proton beam on a nuclear target, as determined by NA3

Intrinsic Charm Distributions

Peak of the J/ψ x_F distribution is within the SeaQuest coverage

p_T distribution, shown for the first time, has a long tail, harder than the pQCD distribution for $\sqrt{s_{NN}} = 15.4$ GeV; at higher energies and especially close to $x_F \sim 0$, the pQCD contribution will dominate and drown the intrinsic charm contribution

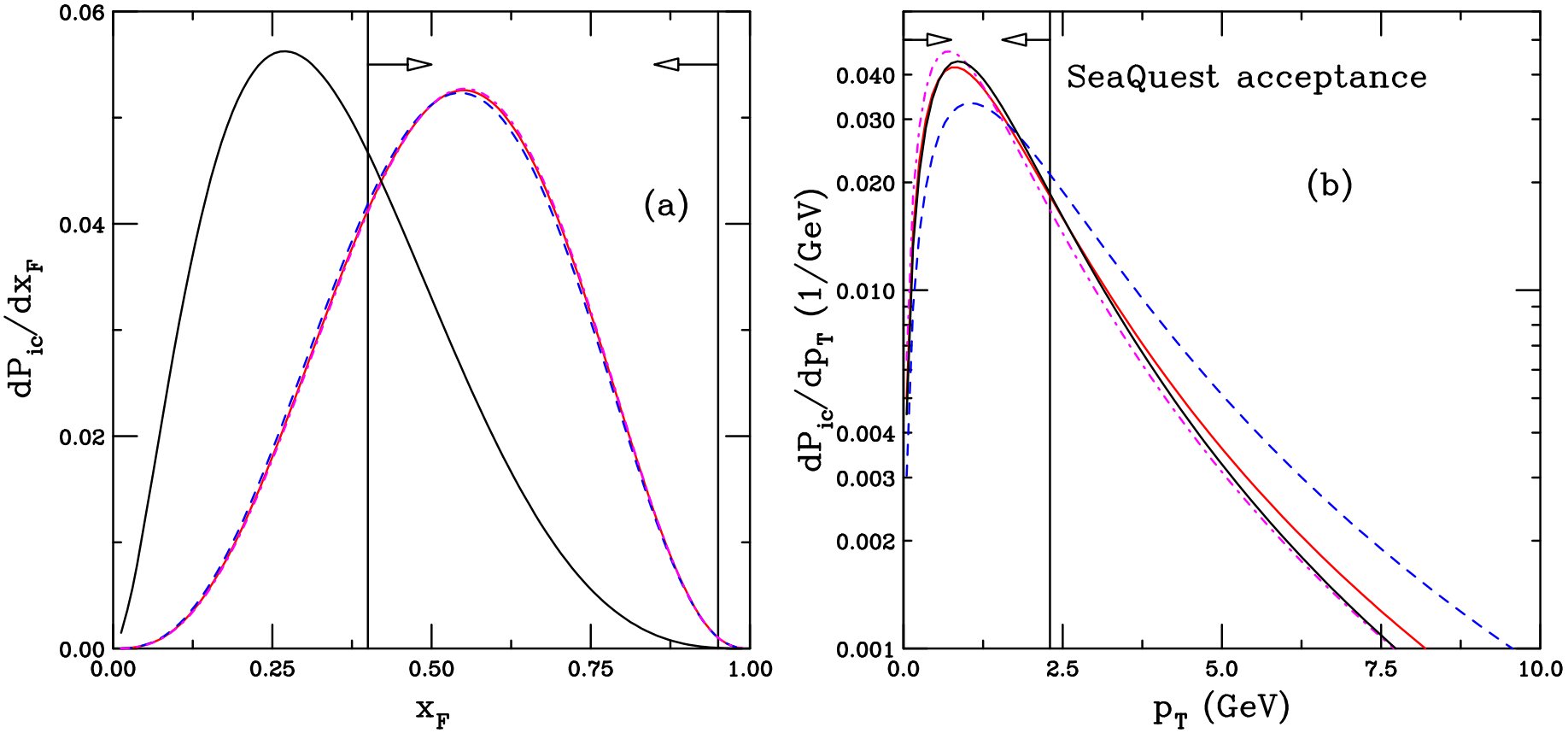

Figure 6: The probability distributions for J/ψ production from a five-particle proton Fock state as a function of x_F (a) and p_T (b). The results are shown for different values of the k_T range for the light and charm quarks. The red curve employs the default values, $k_q^{\max} = 0.2$ GeV and $k_c^{\max} = 1.0$ GeV while the blue dashed curve increases $k_q^{\max}$ and $k_c^{\max}$ by a factor of two and the dot-dashed magenta curve employs half the values of $k_q^{\max}$ and $k_c^{\max}$. The solid black curve shows the x and p_T distributions for a single charm quark from the state.

Evolution of Results vs. x_F for $p + \mathrm{W}$: No Intrinsic Charm

Upper curves do not include absorption, lower curves employ $\sigma_{\mathrm{abs}} = 9$ mb

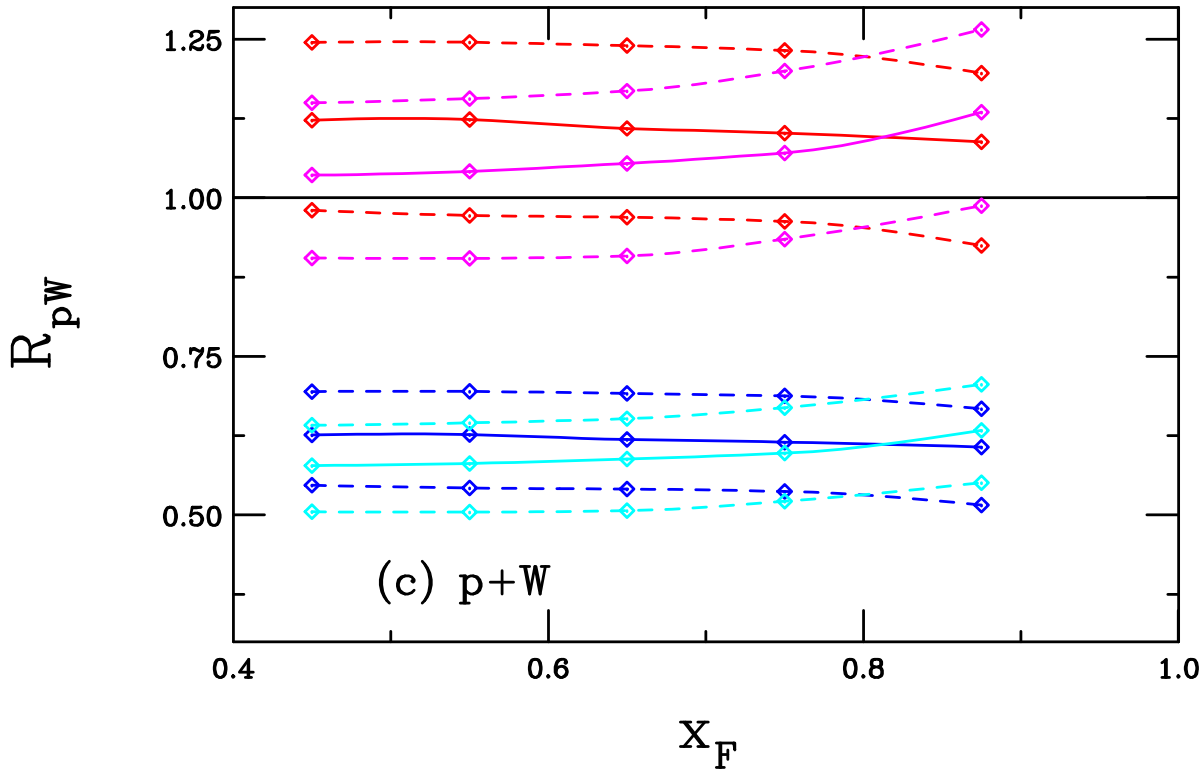

Figure 7: The nuclear modification factors for J/ψ production in SeaQuest as a function of x_F for pQCD production alone for tungsten targets relative to deuterium. Results are shown for nPDF effects alone (red), nPDFs with an additional k_T kick (magenta), nPDFs and absorption (blue), and nPDFs, absorption and k_T broadening (cyan). The solid lines shown the results with the central EPPS16 set while the dashed curves denote the limits of adding the EPPS16 uncertainties in quadrature.

Evolution of Results vs. x_F for $p + \mathrm{W}$: Intrinsic Charm, No Absorption

Intrinsic charm probabilities of 0.1% (top), 0.31% (middle) and 1% (bottom)

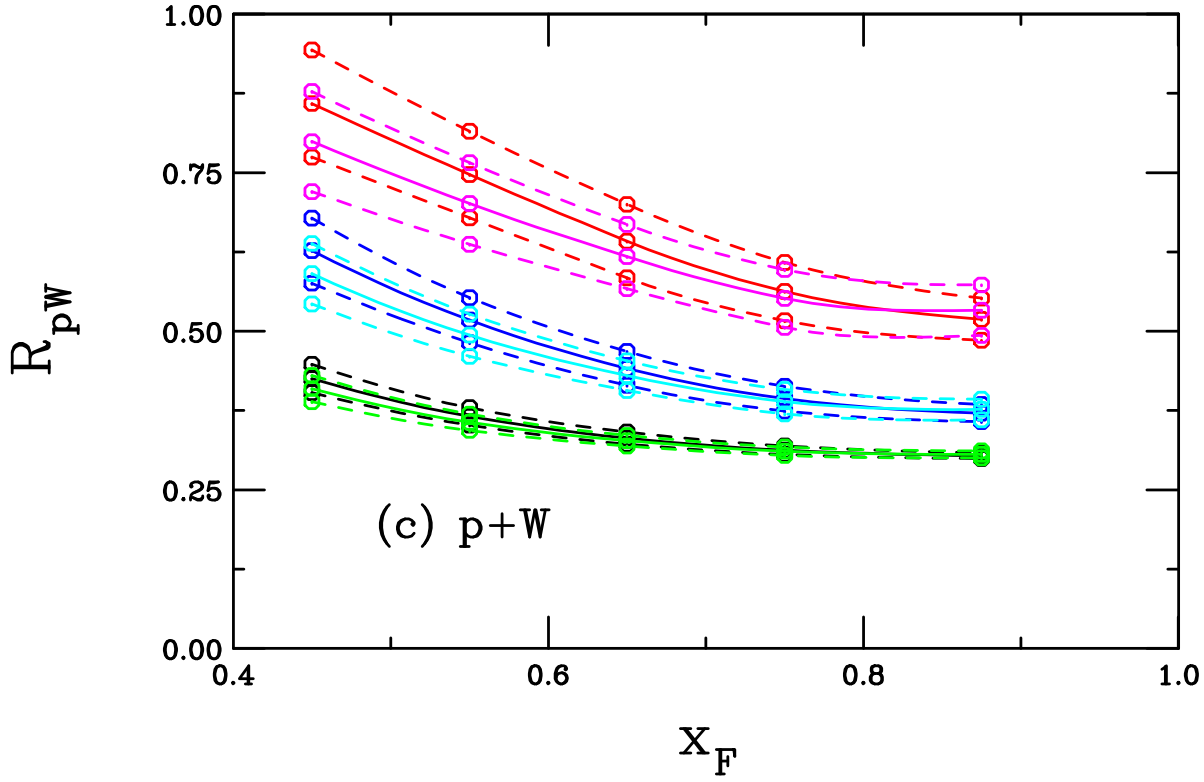

Figure 8: The nuclear modification factors for J/ψ production in SeaQuest as a function of x_F for the combined pQCD and intrinsic charm cross section ratios for tungsten targets relative to deuterium. All calculations are shown with $\sigma_{\mathrm{abs}} = 0$. Results with nPDF effects and the same k_T in $p + \mathrm{d}$ and $p + A$ are shown in the red, blue and black curves while nPDF effects with an enhanced k_T kick in the nucleus are shown in the magenta, cyan and green curves. The probability for IC production is 0.1% in the red and magenta curves; 0.31% in the blue and cyan curves; and 1% in the black and green curves. The solid lines show the results with the central EPPS16 set while the dashed curves denote the limits of adding the EPPS16 uncertainities in quadrature.

Evolution of Results vs. x_F for $p + \mathrm{W}$: Absorption and Intrinsic Charm

Intrinsic charm probabilities of 0.1% (top), 0.31% (middle) and 1% (bottom); $\sigma_{\mathrm{abs}} =$ 9 mb included – truth is likely somewhere between

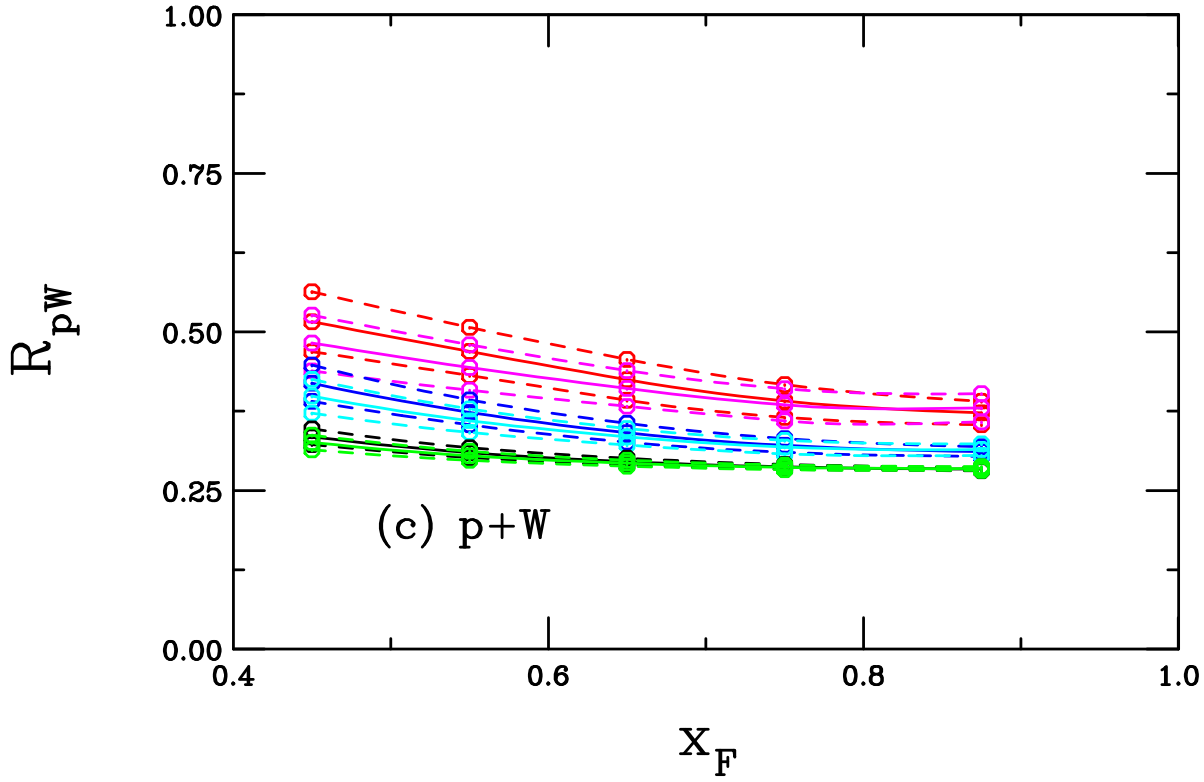

Figure 9: The nuclear modification factors for J/ψ production in SeaQuest as a function of x_F for the combined pQCD and intrinsic charm cross section ratios for tungsten targets relative to deuterium. All calculations are shown with nuclear absorption included. Results with EPPS16 and the same k_T in $p + \mathrm{d}$ and $p + A$ are shown in the red, blue and black curves while EPPS16 with an enhanced k_T kick in the nucleus are shown in the magenta, cyan and green curves. The probability for IC production is 0.1% in the red and magenta curves; 0.31% in the blue and cyan curves; and 1% in the black and green curves. The solid lines shown the results with the central EPPS16 set while the dashed curves denote the limits of adding the EPPS16 uncertainties in quadrature.

Evolution of Results vs. x_F for $p + \mathrm{W}$: All Results Together

The large x_F contribution from intrinsic charm changes the x_F dependence from effectively flat to decreasing with x_F

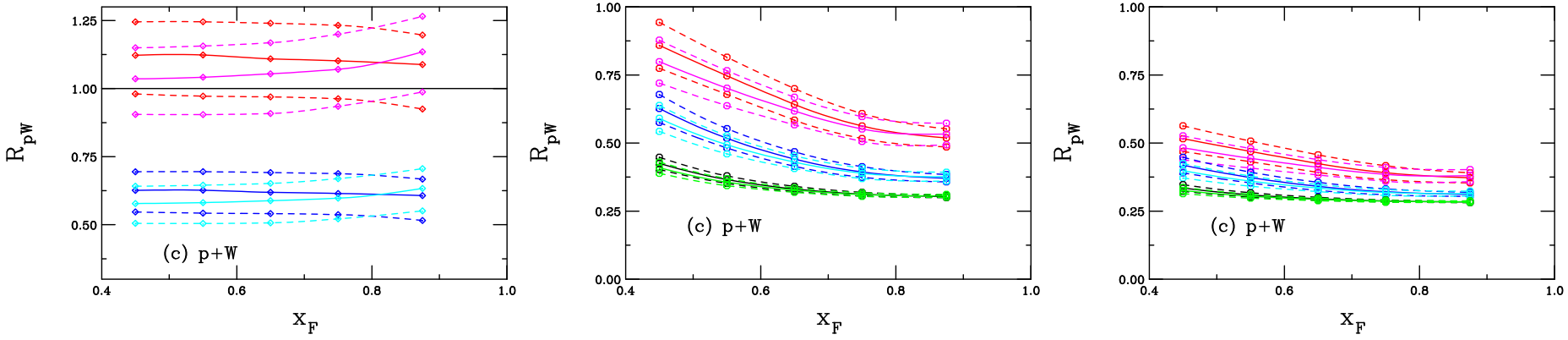

Evolution of Results vs. p_T for $p + \mathrm{W}$: No Intrinsic Charm

Upper curves do not include absorption, lower curves employ $\sigma_{\mathrm{abs}} = 9$ mb

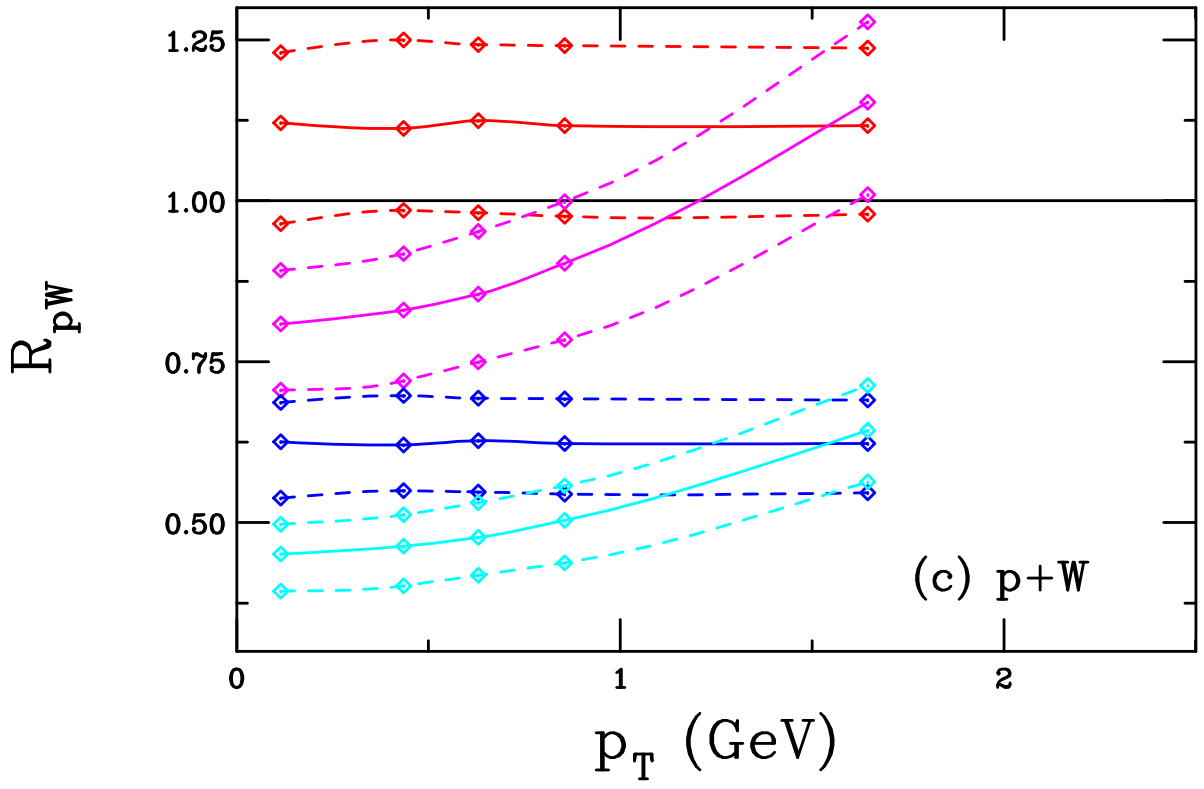

Figure 10: The nuclear modification factors for J/ψ production in SeaQuest as a function of p_T for pQCD production alone for tungsten targets relative to deuterium. Results are shown for nPDF effects alone (red), nPDFs with an additional k_T kick (magenta), nPDFs and absorption (blue), and nPDFs, absorption and k_T broadening (cyan). The solid lines shown the results with the central EPPS16 set while the dashed curves denote the limits of adding the EPPS16 uncertainties in quadrature.

Evolution of Results vs. p_T for $p + \mathrm{W}$: Intrinsic Charm, No Absorption

Intrinsic charm probabilities of 0.1% (top), 0.31% (middle) and 1% (bottom)

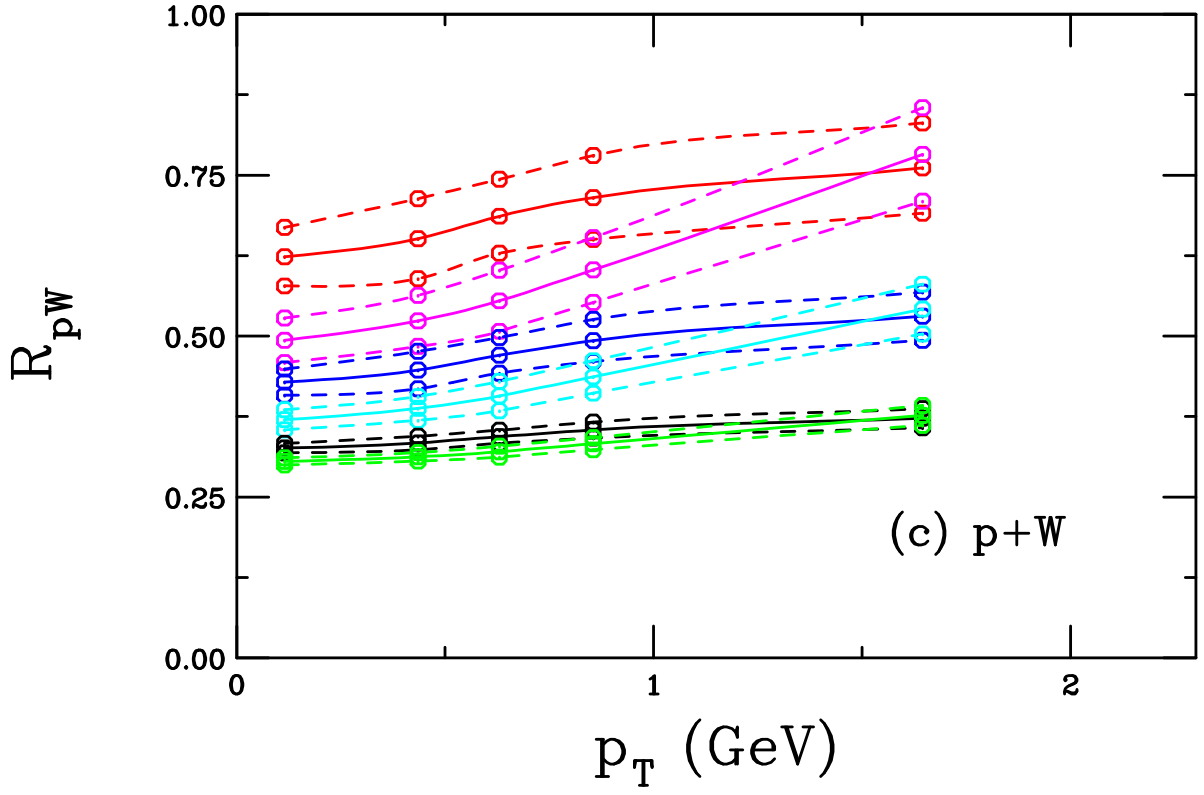

Figure 11: The nuclear modification factors for J/ψ production in SeaQuest as a function of p_T for the combined pQCD and intrinsic charm cross section ratios for tungsten targets relative to deuterium. All calculations are shown with $\sigma_{\mathrm{abs}} = 0$. Results with nPDF effects and the same k_T in $p + \mathrm{d}$ and $p + A$ are shown in the red, blue and black curves while nPDF effects with an enhanced k_T kick in the nucleus are shown in the magenta, cyan and green curves. The probability for IC production is 0.1% in the red and magenta curves; 0.31% in the blue and cyan curves; and 1% in the black and green curves. The solid lines show the results with the central EPPS16 set while the dashed curves denote the limits of adding the EPPS16 uncertainities in quadrature.

Evolution of Results vs. p_T for $p + \mathrm{W}$: Absorption and Intrinsic Charm

Intrinsic charm probabilities of 0.1% (top), 0.31% (middle) and 1% (bottom); $\sigma_{\mathrm{abs}} =$ 9 mb included – truth is likely somewhere between

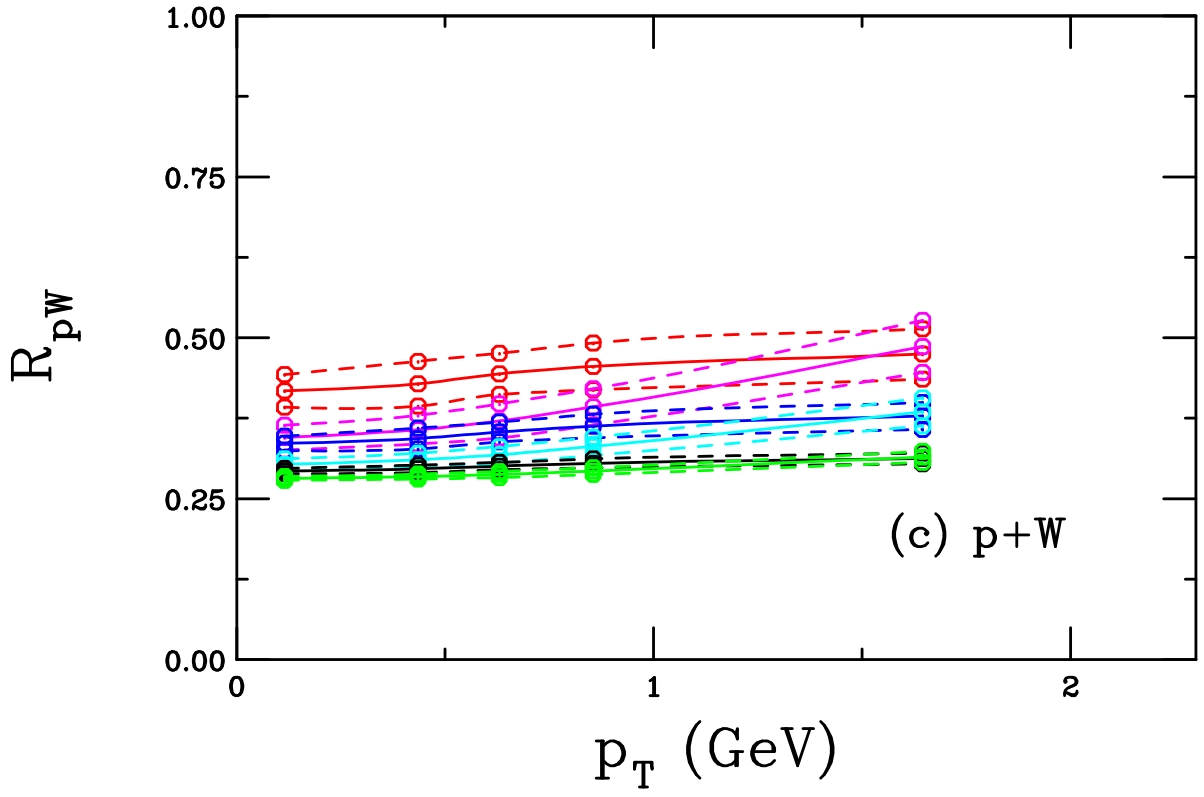

Figure 12: The nuclear modification factors for J/ψ production in SeaQuest as a function of p_T for the combined pQCD and intrinsic charm cross section ratios for tungsten targets relative to deuterium. All calculations are shown with nuclear absorption included. Results with EPPS16 and the same k_T in $p + \mathrm{d}$ and $p + A$ are shown in the red, blue and black curves while EPPS16 with an enhanced k_T kick in the nucleus are shown in the magenta, cyan and green curves. The probability for IC production is 0.1% in the red and magenta curves; 0.31% in the blue and cyan curves; and 1% in the black and green curves. The solid lines shown the results with the central EPPS16 set while the dashed curves denote the limits of adding the EPPS16 uncertainties in quadrature.

Evolution of Results vs. x_F for $p + \mathrm{W}$: All Results Together

Intrinsic charm dominantes the SeaQuest acceptance region

Absorption aids the intrinsic charm dominance but may be overestimated, the value of 9 mb was taken for $x_F \sim 0$ so it could be lower in the forward region

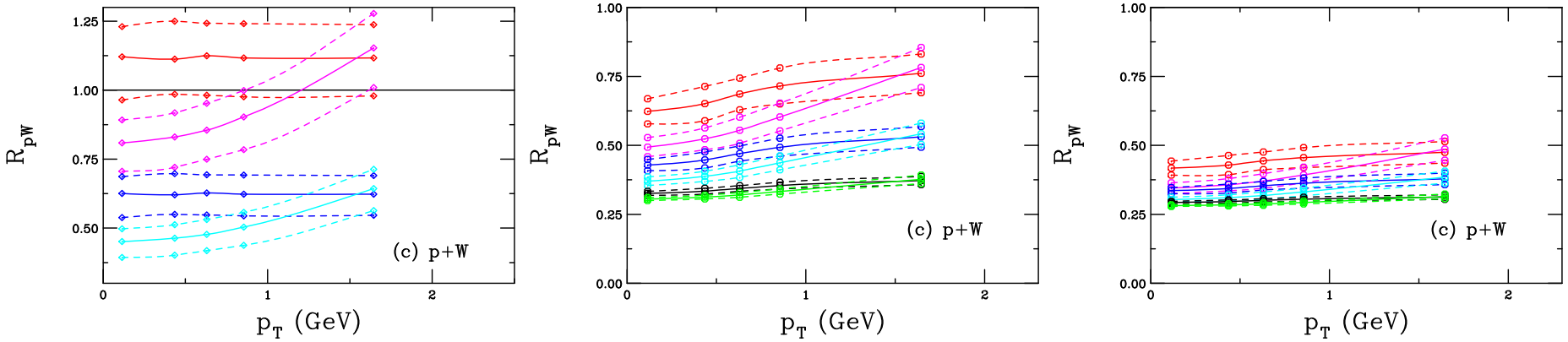

Comparison with α Extracted from E866 J/ψ Data

Update on previous calculations (PRC 61, 035203 (2000)), now with p_T ratios

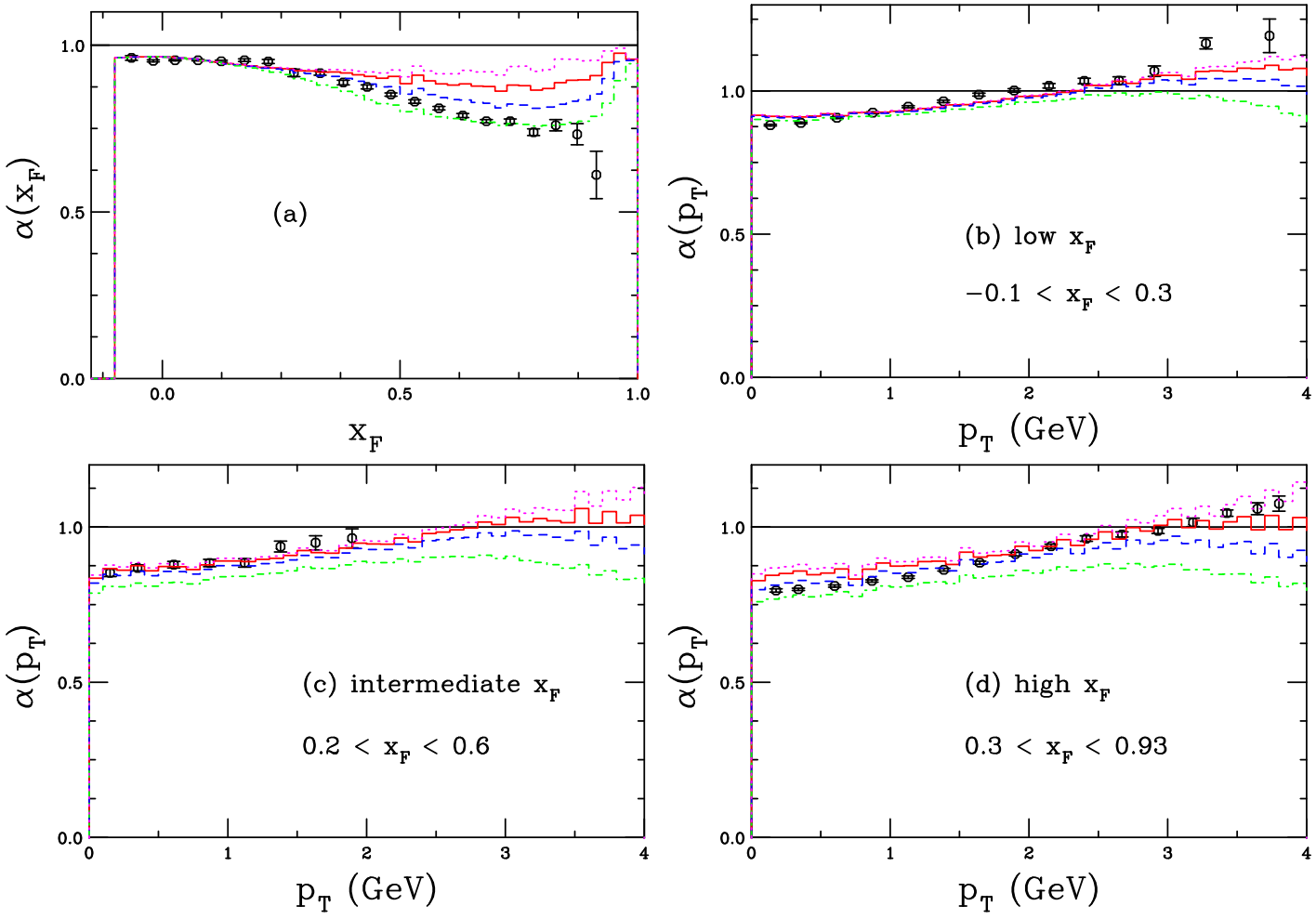

Figure 13: The exponent $\alpha(x_F)$ (a) and $\alpha(p_T)$ for low x_F (b), intermediate x_F (c), and high x_F (d). The dotted magenda curves use $P^0_{\mathrm{ic}\,5} = 0$ while the solid red, dashed blue, and dot-dashed green curves show $P^0_{\mathrm{ic}\,5} = 0.1\%$, 0.31% and 1% respectively. The E866 data (PRL **84**, 3256 (2000)) are the black points.

Summary

The SeaQuest experiment is in a good position to study J/ψ production where intrinsic charm should be dominant

The final SeaQuest J/ψ data, combined with an analysis of the perturbative and intrinsic charm contributions, could determine the probability of J/ψ production from intrinsic charm